Heliyon 9 (2023) e17610

Contents lists available at ScienceDirect

Heliyon

journal homepage: www.cell.com/heliyon

A three orders of magnitude increase in nonlinear optical response by external electric field on Cryptand[2.2.2] (C222) based alkaline earthides

Annum Ahsan [a], Faiza Fayyaz [a], Sehrish Sarfaraz [a], Malai Haniti S.A. Hamid [b], Natasha A. Keasberry [b], Khurshid Ayub [a,**], Nadeem S. Sheikh [b,*]

[a] Department of Chemistry, COMSATS University Islamabad, Abbottabad Campus, Abbottabad, KPK, 22060, Pakistan
[b] Chemical Sciences, Faculty of Science, Universiti Brunei Darussalam, Jalan Tungku Link, Gadong, BE1410, Brunei Darussalam

ARTICLE INFO

Keywords:
Alkaline earthides
NLO materials
Excess electron
Hyperpolarizability (β_o)
Vertical ionization potential

ABSTRACT

A new series of alkaline earthides based on Cryptand [2.2.2] (C222) containing nine complexes is designed by carefully placing alkali metals and alkaline earth metals inside and outside the C222 complexant, respectively *i.e.,* M1(C222)M2 (M1 = Li, Na, K; M2 = Be, Mg, Ca). The designed complexes are reasonably stable both electronically and thermodynamically, as revealed through their vertical ionization potentials (VIPs) and interaction energies, respectively. Moreover, the true alkaline earthide nature of the complexes is confirmed through NBO and FMO analyses showing the negative charges and HOMOs over the alkaline earth metals, respectively. The further validity of true earthide characteristic is represented graphically by the spectra of partial density of states (PDOS). HOMO-LUMO gaps of the compounds are also very small (from 2.23 to 2.83 eV) when compared with pure cage's (C222) H-L gap *i.e.,* 5.63 eV. All these features award these complexes with very small values of transition energies (ΔE) ranging from 0.68 to 2.06 eV ultimately resulting in remarkably high hyperpolarizability values up to 2.7×10^5 au (for $Na^+(C222)Mg^-$). Furthermore, applying external electric field (EEF) on the complexes enhances hyperpolarizability further. A remarkable increase of 1000 folds has been seen when hyperpolarizability of $K^+(C222)Ca^-$ is calculated after EEF application *i.e.*, from 8.79×10^4 au to 2.48×10^7 au; when subjected to 0.001 au external electric field.

1. Introduction

Design of nonlinear optical (NLO) materials has been the subject of significant scientific research for the last several decades [1] due to their potential uses in various fields [2–7] *i.e.,* optical communication [8], optical computing [4,9], laser devices [10], nonlinear microscopy [11], photocatalysis [12] and optical limiting applications [13,14] *etc*. In this regard, numerous approaches have been proposed for not just designing new NLO substances but to improve already proposed materials' nonlinear optical responses. These approaches include diradical character [15,16], donor-π-acceptor systems [17], the anionic group theory [18,19], synthesis of octupolar molecules [20], systems with excess electrons [21–28] *etc.* Li et al., in 2004 studied the compounds containing excess

* Corresponding author.
** Corresponding author.
E-mail addresses: khurshid@cuiatd.edu.pk (K. Ayub), nadeem.sheikh@ubd.edu.bn (N.S. Sheikh).

https://doi.org/10.1016/j.heliyon.2023.e17610
Received 18 May 2023; Received in revised form 22 June 2023; Accepted 22 June 2023
Available online 24 June 2023

electrons showing remarkable NLO response [29,30]. Since then, introduction of excess electron into the structure of a compound is considered as an excellent approach for the purpose of boosting of a system's NLO response.

A large number of different excess electron compounds have been designed subsequently. Electrides [31–33] are one of the commonly studied excess electron compounds with significantly higher NLO response. Their design principle includes an electron source (mostly an alkali metal) intercalated into the complexant as source of excess electron and an excess electron acting as anion lying over the complexant. There are different types of electrides studied with different electron sources and complexants up till now. For example, Cs^+(18-crown-6)2e^- is the first electride with Cs and 18-crown-6 ether acting as excess electron source and complexant, respectively [34]. Similarly, M^+(cryptand [2.2.2])e^- is the electride with alkali metals like Li, Na and K as source of excess electron and cryptand[2.2.2] as a complexant [35,36]. Moreover, M^+(15-crown-5)e^- [37], Na^+(tri-pip-aza222)e^- [38], Na^+(calix [4]pyrrole)e^- [39], AM3@GDY (AM = Li, Na, K) [40] *etc.* electrides have been reported. Another class of excess electron compounds is alkalides with remarkable NLO response. Alkalides are the compounds that contain atoms intercalated into the complexant (most probably the alkali metals) as sources of excess electrons and another alkali metal present outside the complexant acting as an electron acceptor (donated by the intercalated atom). The electron acceptor alkali metal atom converts into alkali metal anion and contains excess electron of the system [41–45] such as $M^+(n^6Adz)M^-$ [46], M^+(calix [4]pyrrole)M^- (in these compounds alkali metal cations and alkali metal anions are represented by M^+ & M^- respectively) [47] *etc.*

Recently, a new type of compounds having excess electron has been proposed. They comprise of alkali metals as electron donors (cations) with alkaline earth metals as electron acceptors (anions). The position of alkali metals and alkaline earth metals in these compounds are at the inner side and outer side of the complexant, respectively. With $C_6H_6F_6$ as a complexant ($Li(C_6H_6F_6)M$ (in which M = Be, Mg and Ca)) [48], the alkaline earthides were designed for the first time showing significantly higher NLO response. Our group has been working on these compounds and have designed a number of alkaline earthides with different complexant molecules *i.e.,* $M^+(NH_3)_6M^-$ [49], $M^+(3^6Adz)M^-$ [50], $M^+(2^6Adz)M^-$ [51], M^+(calix [4]pyrrole)M^- [52], M^+(15-crown-5 ether)M^- [53] (here, alkali metals are represented by M^+ while alkaline earth metals are represented by M^-). The designed earthides have shown remarkable NLO response which has motivated us to explore them further. We have selected yet another complexant *i.e.,* cryptand [222] (C222) for the new series of alkaline earthides. It's a bicyclic compound and is known for its high affinity for alkali metal cations. Literature reveals many examples where C222 is used as an encapsulating agent for alkali metals [54]. This feature of C222 can be very useful for us in designing alkaline earthides as the basic design principle of alkaline earthides is, encapsulation of alkali metals in the complexant with alkaline earth metals kept outside the complexant. Moreover, the structure of cryptand[2.2.2] that we have utilized in our study also contains a benzene ring, as highlighted in Fig. 1(a and b). Presence of the ring is expected to influence the complexation behavior and overall flexibility of the complexant (the flexibility gets reduced) [55]. C222 contains a three-dimensional interior cavity which provides a binding site for the "guest" ions with the benzene ring allowing the electrostatic attractive forces to develop between the complexed ions and the π-electrons [56] thus making it better complexating agent.

Furthermore, we did a complete investigation on the effects of external electric field on the hyperpolarizability of designed series of alkaline earthides. As application of external electric field results in an increased charge transfer from alkali metal to alkaline earth metal as well as decreases the energy gap of the alkaline earthides hence enhances the hyperpolarizability of alkaline earthides [52,57,58].

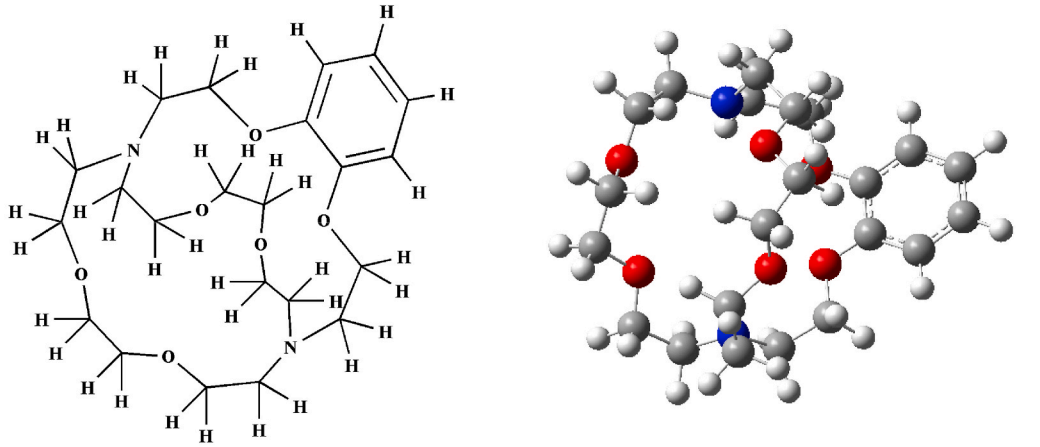

Fig. 1. Cryptand[2.2.2] chemdraw (a) and GaussView (b) structure.

2. Computational methodology

One of the DFT-D functionals *i.e., ωB97X-D* (a hybrid) with distinctive features like long range and dispersion correction is used in the current study. It is reported to be a suitable functional for complexes with alkali metals [59] and gives reliable results for the study of thermochemistry, non-covalent bonding interactions [51,60,61] and transfer of charge within compounds. As the charge transfer and long-range interactions are the prominent features of the systems that we have designed in the current study, hence they demand the functional like *ωB97X-D* for reliable results. Therefore, *ωB97X-D* functional is employed (along with 6-31G+(d,p)). Moreover, other reasons for selecting *ωB97X-D* are the literature reports which show that the results of nonlinear optical studies by *ωB97X-D* are comparable to coupled cluster methods' (CCSD(T)) results, that is acknowledged in quantum chemistry as a "gold standard" method [62]. Historically, the coupled-cluster methods have been used for the accurate estimation of polarizability and hyperpolarizability but its usage as a routine computational tool for screening is limited by its greater computational cost. Contrariwise, density functional theory (DFT) methods possess favorable balance between computational cost and accuracy which has enabled them gain more attention. But the calculation of β values through DFT methods is functional-dependent. This is because of different exchange-correlation potentials of every functional. It is well known that the exchange correlation part is very important for calculation of NLO properties. So, CCSD(T) calculations are used as a suitable benchmark for comparing NLO properties obtained through DFT (by employing a number of range-separated exchange functionals) [62]. As the systems under study are large for which CCSD (T) calculations are not very practical hence DFT methods are chosen in our study on the basis of the results obtained from comparison with CCSD(T). According to the results of comparison study, *ωB97X-D* functional shows results comparable to coupled cluster

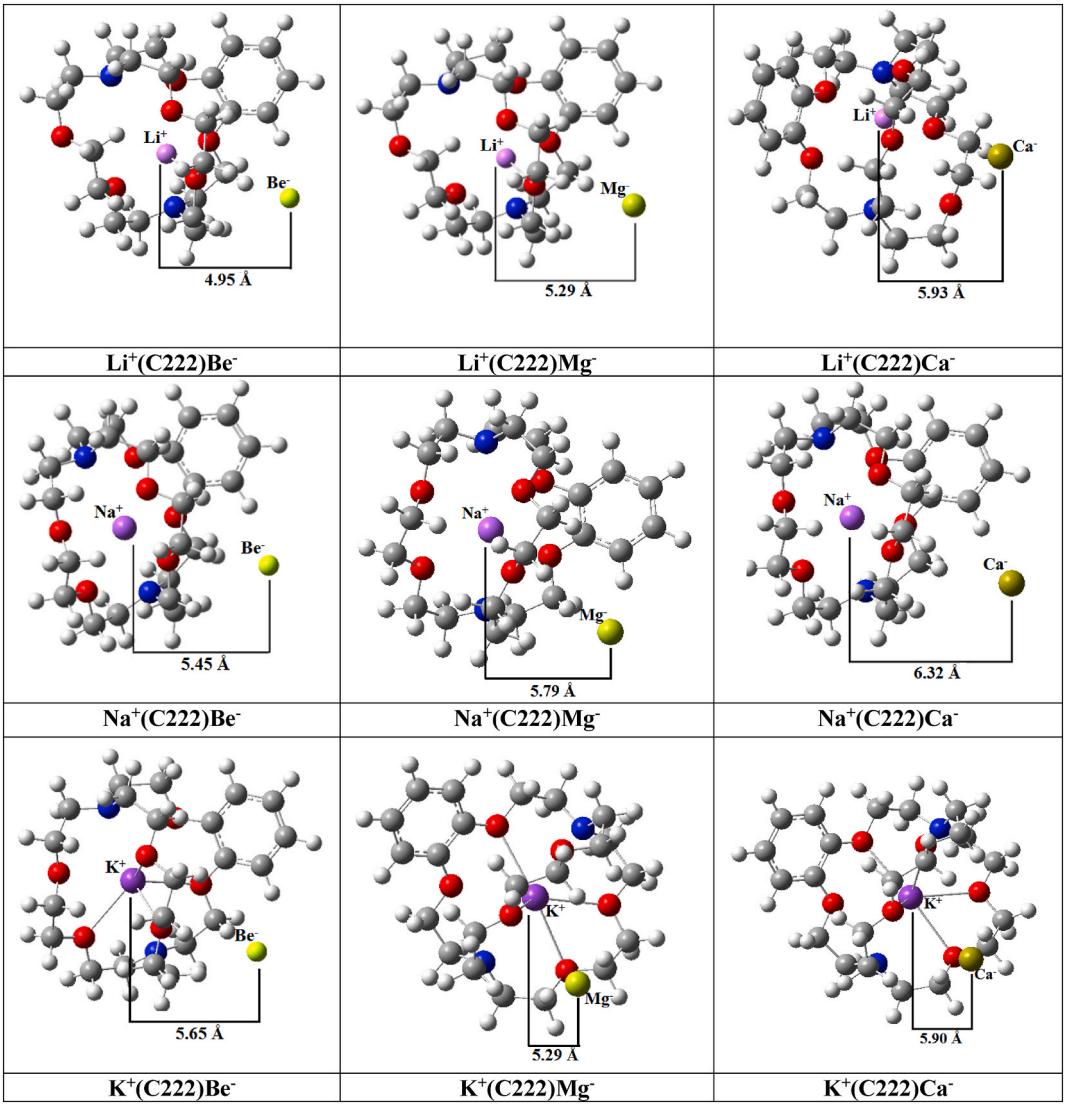

Fig. 2. Optimized Geometries of M1(C222)M2 (where M1 = Li, Na, K; M2 = Be, Mg, Ca) compounds calculated at *ωB97X-D*/6-31+G (d,p) level.

methods' results [63]. Furthermore, as per the reported studies, authentic study of hyperpolarizability demands range separation to be the feature of the functional to be employed. Hence, *ωB97X-D* is an authentic choice to be made as it contains 100% of long-range exact exchange, a small fraction (about 22%) of short-range exact exchange [32,63–68], a modified B97 exchange density functional for short-range interaction and empirical dispersion corrections. Empirical dispersion correction is an additional term which is based on Grimme's D2 dispersion model [9,61,69–72].

Gaussian 09 program package is used for performing all the DFT simulations [73] whereas for the visualization of optimized geometries GaussView 5.0 is used [74]. The geometries of the designed compounds are optimized first. Then, comprehensive study of electronic properties is done that includes estimation of NBO (natural bond orbitals) and gap between HOMO and LUMO (HOMO--LUMO gaps). Further, spectra are generated for the partial densities of states (PDOS) to verify the electronic properties further through multiwfn [75].

For the detailed study, at *ωB97X-D*/6-31G+(d,p), vertical ionization potential (VIP), dipole moments (μ_o), ultra-violet–visible–infrared absorption spectra, isotropic polarizability and the first hyperpolarizability are analyzed.

The change in the NLO response on application of external electric field (EEF) has been figured out by repeating the calculations (Optimization, NBO, Hyperpolarizability, Energy gap) under external electric field (EEF) having the strength equal to 0.001 au along the charge transfer direction *i.e.*, M1→ M2.

In order to get the oscillator strength (f_o), crucial excitation energies (ΔE) and change in dipole moment (Δμ), the time-dependent DFT calculations are performed at TD-*ωB97X-D*/6-31+G(d,p) level of theory. The time dependent DFT calculations are carried out for all the designed compounds in order to obtain the state to which summation is restricted (called as the crucial excited state) in two level model. Systems with numerous electrons show a number of possible electronic excitations. However, the dipole allowed transitions are only a few because of the symmetry and selection rule. Only these dipoles allowed transitions contribute to some associated properties of the molecule. In the current study, after considering 20 electronic states, we have applied FSM *i.e.,* few state model. It gives us the states showing considerable contribution (dipole allowed transitions) to NLO. FSM works by eliminating those states which show lesser contribution or zero contribution to the NLO properties in SOS formula. In this way, just evaluating the dipole allowed transitions in SOS formula decreases the computing cost considerably. This is because of the fact that there are only a few dipole allowed transitions in electronic spectra [76,77]. Out of all these 20 excited states, we consider the electronic state with maximum value of oscillator strength (f_o) as the main electronic transition contributing most to NLO response (crucial excited state). This particular excited state's transition energy (ΔE) is also taken as one of the controlling factors of hyperpolarizability.

3. Results and discussion

3.1. Geometrical characteristics

The optimization of geometries of M1(C222)M2 is carried out first. The final optimized structures (given in Fig. 2) are such that they contain alkali metals at the internal face of C222 complexant while the external face of C222 complexant contains alkaline earth metals (interacting with hydrogens of complexant). Interaction distance between the metal ions is calculated (Table 1). The interaction distance shows an increase when alkali metal cation (M1) present inside the C222 (complexant) is same while alkaline earth metal (M2) situated outside the C222 (complexant) is changed. Li and Na series follow this increase in interaction distance trend. For Li^+(C222)M2 series (M2 represents Be, Mg and Ca), the distance between metals/interaction distance increases in the order; Li^+ - Be^- (having distance in between them equal to 4.95 Å) < Li^+ - Mg^- (with the distance 5.29 Å) < Li^+ - Ca^- (with the distance 5.93 Å). A similar trend is exhibited by next series *i.e.,* the Na series (Na^+(C222)M2) where Na^+ - Be^- (with the distance 5.45 Å) < Na^+ - Mg^- (with the distance 5.79 Å) < Na^+ - Ca^- (with the distance 6.32 Å). The increase in interaction distance is on account of the size enlargement of the alkaline earth metals along with enhancement in their electropositive nature which ultimately decreases the interaction between the metals [49,51,76]. While for K series, K^+(C222)M2, the increase is not monotonic. The reason may be the larger size of K which slightly distorts the complexants cage structure. The trend followed by this series is; K^+ - Mg^- (with the distance 5.29 Å) < K^+ - Be^- (with the distance 5.65 Å) < K^+ - Ca^- (with the distance 5.90 Å).

Table 1
NBO charges on M1 (Q_{M1} in |e|) and M2 (Q_{M2} in |e|), symmetries, vertical ionization potential, VIP (eV), distances between M1 and M2, (in Å), ground state dipole moments, μ_o (D) and energy gaps, H-L gaps (eV) in the M1(C222)M2 compounds.

M1(C222)M2	Q_{M1}	Q_{M2}	Sym.	VIP	$d_{M1\text{-}M2}$	μ_o	E_H	E_L	H-L gap
Li^+(C222)Be^-	0.57	−0.81	C_1	4.65	4.95	15.48	4.65	4.36	2.83
Li^+(C222)Mg^-	0.57	−0.83	C_1	4.64	5.29	17.09	4.64	4.36	2.53
Li^+(C222)Ca^-	0.85	−0.77	C_1	4.59	5.93	19.52	4.59	4.34	2.37
Na^+(C222)Be^-	0.62	−0.83	C_1	4.61	5.45	17.78	4.61	4.36	2.56
Na^+(C222)Mg^-	0.53	−0.85	C_1	4.60	5.79	19.58	4.60	4.35	2.26
Na^+(C222)Ca^-	0.87	−0.71	C_1	4.60	6.32	21.50	4.60	4.35	2.26
K^+(C222)Be^-	0.65	−0.85	C_1	4.58	5.65	18.53	4.58	4.36	2.29
K^+(C222)Mg^-	0.61	−0.83	C_1	4.56	5.29	16.84	4.56	4.34	2.23
K^+(C222)Ca^-	0.88	−0.77	C_1	4.56	5.90	19.20	4.56	4.34	2.24

HOMO	LUMO
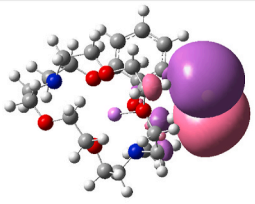	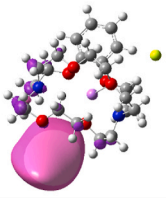
$Li^{+}(C222)Be^{-}$	
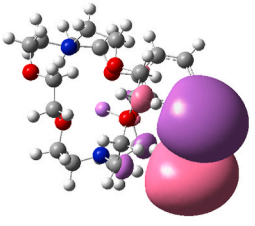	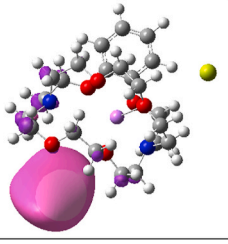
$Li^{+}(C222)Mg^{-}$	
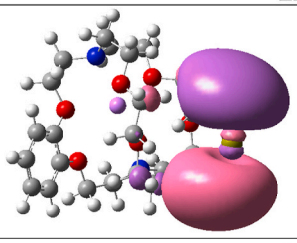	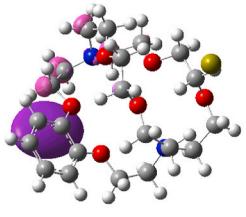
$Li^{+}(C222)Ca^{-}$	
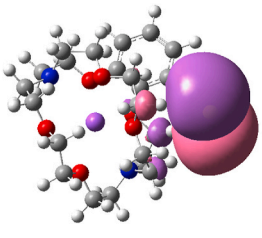	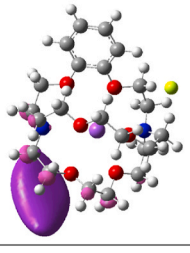
$Na^{+}(C222)Be^{-}$	
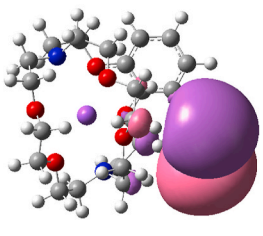	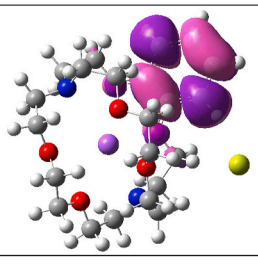
$Na^{+}(C222)Mg^{-}$	
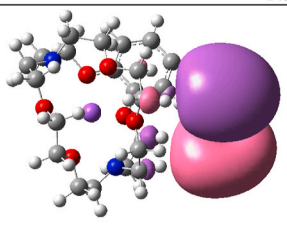	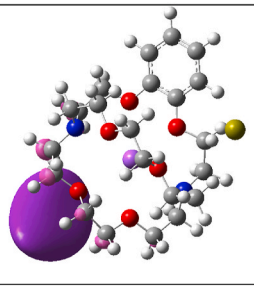
$Na^{+}(C222)Ca^{-}$	

(caption on next page)

Fig. 3. HOMOs and LUMOs of Li^+(C222)M2 and Na^+(C222)M2 compounds (M2 = Be, Mg, Ca) plotted at isovalue of 0.02.

3.1.1. Dipole moment

In Table 1, the dipole moment of designed compounds is presented. As dipole moment is the vector product of two parameters, one is the magnitude of charges and other is the distance between those charges. There is a direct relation between both these parameters and the dipole moment. The direct relation of dipole moment with distance between the charges can be observed through the values of dipole moment calculated for Li^+(C222)M2 and Na^+(C222)M2 series. The complexes of both these series show an increase in dipole moment by size enlargement of anion (as a result of size enlargement of alkaline earth metal, overall distance between the charges

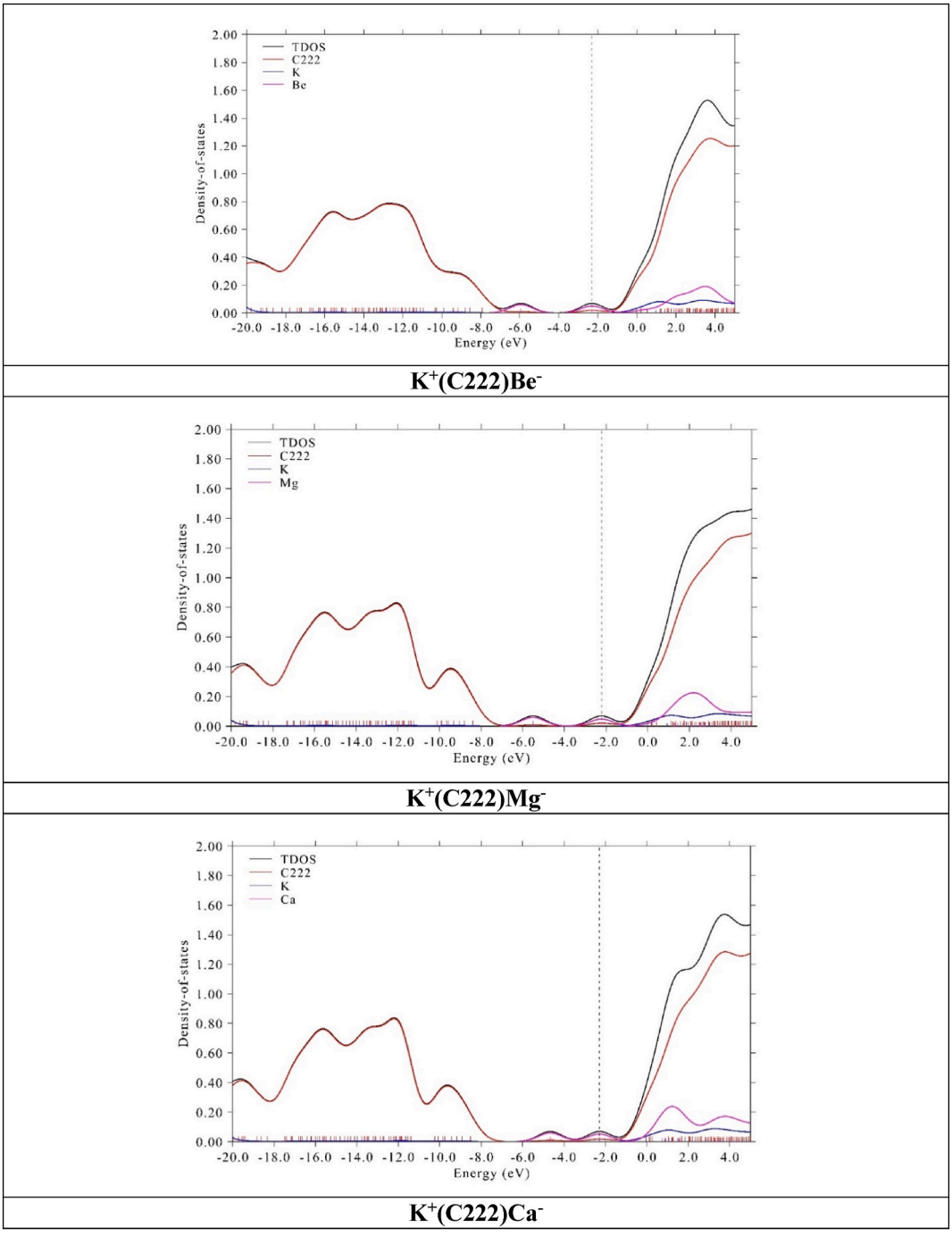

Fig. 4. Spectra of partial density of states (PDOS) for K^+(C222)M2 (M2 = Be, Mg, Ca) compounds.

increase). For Li^+(C222)M2 series, dipole moment of Li^+(C222)Be^- (15.48 D) < Li^+(C222)Mg^- (17.09 D) < Li^+(C222)Ca^- (19.52 D). Similarly, for Na^+(C222)M2 series, dipole moment of Na^+(C222)Be^- (17.78 D) < Na^+(C222)Mg^- (19.58 D) < Na^+(C222)Ca^- (21.50 D). For the K series, dipole moment of the series does not increase in regular order. The reason behind such a trend is interaction distance between the metal atoms. The distance between metal atoms do not increase in a regular pattern (like Li and Na series) when size of alkaline earth metal increases. For this series, the trend followed by interaction distance and dipole moment is, K^+ - Mg^- < K^+ - Be^- < K^+ - Ca^-. Therefore, for all the three series, interaction distance between the metal atoms is the deciding factor for dipole moment.

3.2. Electronic properties

In order to confirm that whether the studied compounds have true alkaline earthide nature or not, study of NBOs *i.e.,* natural bond orbitals is carried out. NBOs analyses show that in the designed compounds, alkali metals bear positive charges while the charges developed by alkaline earth metals are negative showing that charge is transferred from alkali metals (donor metal atoms here) to alkaline earth metals (acceptor metal atoms here). In this way, excess electron is inserted into the complex, reposing over the acceptor metal atoms of system (alkaline earth metal). Moreover, alkaline earth metals' negative charge corroborate the designed compounds as having true earthide character.

NBO analyses show that Li^+(C222)M2 series follows a non-monotonic trend of increase of NBO charge (negative charge) on alkaline earth metals *i.e.,* Li^+(C222)Mg^- (−0.83 |e|) > Li^+(C222)Be^- (−0.81 |e|) > Li^+(C222)Ca^- (−0.77 |e|). For Na^+(C222)M2 series, the increase is also of the same order (similar to Li^+(C222)M2 series) *i.e.,* Na^+(C222)Mg^- (−0.85 |e|) > Na^+(C222)Be^- (−0.83 |e|) > Na^+(C222)Ca^- (−0.71 |e|). The Na series shows the highest negative charge in the complex (on alkaline earth metal) having highest hyperpolarizability (similar hyperpolarizability trend is shown by this series). For K^+(C222)M2 series, a decreasing trend is followed from Be toward Ca *i.e.,* K^+(C222)Be^- (−0.85 |e|) > K^+(C222)Mg^- (−0.83 |e|) > K^+(C222)Ca^- (−0.77 |e|).

For validation of earthide nature further, frontier molecular orbitals (FMOs) are viewed which show the position of HOMO (highest occupied molecular orbital). In the designed complexes, position of HOMO is over alkaline earth metal (Fig. 3/Fig. S1). Hence, validating the alkaline earthide nature. Moreover, PDOS (partial density of states) spectra are also generated (Fig. 4/Fig. S2) for confirmation of position of HOMO. The spectra clearly show the HOMOs of all the complexes repose over alkaline earth metals.

The final geometries contain alkali metals lying at the internal face of C222 complexant while at external face of C222 complexant, alkaline earth metals are present (interacting with hydrogens of complexant). Oxygen atoms (electron rich) of the complexant are oriented toward the metals near them (alkali metals). These oxygen atoms push the electron present in outermost shell of alkali metals (ns^1 electron) which passages toward and finally surrounds the alkaline earth metal.

The gaps between highest occupied and lowest unoccupied molecular orbitals (abbreviated as H-L gaps) are calculated and the designed compounds show H-L gaps as very small (from 2.23 to 2.83 eV) when compared with pure cage's (C222) H-L gap *i.e.,* 5.63 eV. There is clear reduction in value that is credited to the position of excess electron *i.e.,* alkaline earth metal, in case of alkaline earthide complexes. Discussing the H-L gaps series wise, we see that there is reduction in H-L gap with the alkaline earth metal anion's enlargement. For Li^+(C222)M2 and Na^+(C222)M2 series, H-L gap decreases monotonically like, Li^+(C222)Be^- (with 2.83 eV energy gap) > Li^+(C222)Mg^- (with 2.53 eV energy gap) > Li^+(C222)Ca^- (with 2.37 eV energy gap) and Na^+(C222)Be^- (with 2.56 eV energy gap) > Na^+(C222)Mg^-/Na^+(C222)Ca^- (with 2.26 eV energy gap). The larger the size of anion, the lesser its electronegativity and less likely it can hold the electron. This lowers the HOMO-LUMO gap which ultimately causes easier excitation of the excess electron. For K series, irregular trend for H-L gap is followed *i.e.,* K^+(C222)Be^- > K^+(C222)Ca^- > K^+(C222)Mg^-. The lowest H-L gap of this series is observed for K^+(C222)Mg^- complex which has the lowest interaction distance between the interacting metal atoms (among this series). The lower interaction distance may cause the transfer of charge to be better and H-L gap to be lower.

The complexes possess reasonably high values of vertical ionization potential (VIP) (values are given in Table 1). Such higher values impart electronic stability to the complexes. For all the three series, there is influence of size of anion (*i.e.,* alkaline earth metals) on values of VIP. They seem to decrease by increase of anion's size. This is because of the fact that ionization energy becomes lower with increase of anion's size. For Li^+(C222)M2 series, the VIP of Li^+(C222)Be^- (4.65 eV) is greater than Li^+(C222)Mg^- (4.64 eV) which is greater again than Li^+(C222)Ca^- (4.59 eV). A similar trend is followed by Na^+(C222)M2 and K^+(C222)M2 series *i.e.,* VIP of Na^+(C222)Be^- (4.61 eV) > Na^+(C222)Mg^- (4.60 eV)/Na^+(C222)Ca^- (4.60 eV) and VIP of K^+(C222)Be^- (4.58 eV) > K^+(C222)Mg^- (4.56 eV)/K^+(C222)Ca^- (4.56 eV).

Table 2
Calculated mean polarizabilities, α_o (au), mean first hyperpolarizabilities, β_o (au), λ_{max} (nm), transition energies, ΔE (eV), oscillator strengths, f_o, (au) and differences in dipole moments, Δμ (D) between the ground and excited states of the crucial excited states for the M1(C222)M2 compounds.

M1(C222)M2	α_o	β_o	λ_{max}	ΔE	f_o	Δμ
Li^+(C222)Be^-	480	2.4×10^4	1256	0.98	0.07	2.32
Li^+(C222)Mg^-	646	1.0×10^5	1614	0.76	0.10	5.30
Li^+(C222)Ca^-	*735*	1.3×10^5	1506	0.82	0.11	5.23
Na^+(C222)Be^-	492	6.5×10^4	600	2.06	0.06	5.26
Na^+(C222)Mg^-	680	2.7×10^5	1800	0.68	0.08	5.81
Na^+(C222)Ca^-	766	2.0×10^5	1609	0.77	0.11	8.24
K^+(C222)Be^-	507	5.4×10^4	614	2.01	0.09	10.05
K^+(C222)Mg^-	694	1.1×10^5	1796	0.69	0.11	0.01
K^+(C222)Ca^-	423	8.7×10^4	1598	0.78	0.12	0.01

3.3. Nonlinear optical properties

In case of alkaline earthides, a diffuse electron reposes over alkaline earth metal. Due to its diffuse nature, it can easily be excited and renders complexes with significantly lower energies of excitation. Owing to these characteristics, compounds are expected to show larger NLO (nonlinear optical) responses. Therefore, the nonlinear optical properties are calculated. Table 2 contains polarizabilities and first hyperpolarizabilities (α_o and β_o, respectively).

It is observed that the polarizability values of Li series (Li^+(C222)M2) and Na (Na^+(C222)M2) series increase along the series in a monotonic order *i.e.,* α_o increases from Li^+(C222)Be^-/Na^+(C222)Be^- to Li^+(C222)Mg^-/Na^+(C222)Mg^- and further increases from Li^+(C222)Mg^-/Na^+(C222)Mg^- to Li^+(C222)Ca^-/Na^+(C222)Ca^-. Polarizability of both these series shows dependence on alkaline earth metal's size. By the enlargement in alkaline earth metal's size containing excess electron, the polarizability also increases. This is because larger anions have more loosely held electrons in their outermost shell, since they are situated farther away from the nucleus, hence more polarizable. While the K series (K^+(C222)M2) shows a non-monotonic trend of polarizability, showing an increase in value from K^+(C222)Be^- to K^+(C222)Mg^- but further decrease for K^+(C222)Ca^-.

However, the analyses of values of hyperpolarizability of all the three series shows that for Li series (Li^+(C222)M2), β_o increases in a linear pattern, showing an increase in value from Li^+(C222)Be^- to Li^+(C222)Mg^- and then to Li^+(C222)Ca^-. The consistent increase in the value of hyperpolarizability can be credited to alkaline earth metal's size. With the size enlargement of alkaline earth anion, β_o also increases *i.e.,* β_o of Li^+(C222)Ca^- (1.3×10^5 au) > Li^+(C222)Mg^- (1.0×10^5 au) > Li^+(C222)Be^- (2.4×10^4 au). The larger the size of anion, the lesser its electronegativity and it is less likely to hold the electron. This causes easier excitation of the excess electron ultimately increasing β_o.

The β_o of Na and K series, Na^+(C222)M2 and K^+(C222)M2 (M2 = Be, Mg & K), shows a non-monotonic trend. For these two series, β_o increases from Na^+(C222)Be^-/K^+(C222)Be^- to Na^+(C222)Mg^-/K^+(C222)Mg^- but decreases further for Na^+(C222)Ca^-/K^+(C222)Ca^-. The reason behind the elevation in β_o from M1(C222)Be^- to M1(C222)Mg^- (M1 = Na or K) can be alkaline earth metal's size (former compounds contain Be of smaller size and latter contain Mg of greater size). As per the fact that alkaline earth metal atoms in each compound hold the excess electron, the greater the metal's size (holding excess electron), the smaller its ionization energy and the gentler & easier the stimulation of electron from such metal and eventually larger will be the value of hyperpolarizability. So, in this case, alkaline earth metal atom's size (holding excess electron) is the deciding factor for hyperpolarizability value. The value of hyperpolarizability shows decrease further from M1(C222)Mg^- to M1(C222)Ca^- (M1 = Na or K). This can be credited to the increase in interaction distance between the metal ions in a complex. When the interaction distance between the interacting ions becomes the deciding factor for the β_o values, we find the higher hyperpolarizability values for the complexes with smaller distance between the interacting parts. So, in this case the interaction distance is the deciding factor for hyperpolarizability value. Compounds with Mg anion, M1(C222)Mg^- show higher value of hyperpolarizability with shorter distance between interacting ions contrary to the complexes with Ca anion (M1(C222)Ca^-) with greater interaction distance. Na^+(C222)Mg^- (2.7×10^5 au) > Na^+(C222)Ca^- (2.0×10^5 au) > Na^+(C222)Be^- (6.5×10^4 au) and K^+(C222)Mg^- (1.1×10^5 au) > K^+(C222)Ca^- (8.7×10^4 au) > K^+(C222)Be^- (5.4×10^4 au).

3.4. Controlling factors of hyperpolarizability

Certain factors affecting hyperpolarizability *i.e.,* f_o, oscillator strength, Δμ, change in dipole moment and ΔE, energy that is required for transition in between two states *i.e.,* ground and crucial excited state, are studied by employing two level model.

$$\beta_{TL} \approx \Delta\mu \times f_o \,/\Delta E^3$$

The equation shows that there is direct relation of β_o with f_o and Δμ while β_o is related inversely to ΔE^3 (values given Table 2).

The crucial transitions are calculated through the TD-DFT (time dependent density functional theory) calculations. The inverse relation between ΔE and β_o can be observed through the high values of β_o (up to 10^5 au) and the lower values of ΔE (0.68–2.06 eV) for the complexes. Such lower values of ΔE are the reason behind elevated hyperpolarizability values (as confirmed via the previous reports [76,78–80]. Moreover, this inverse relation can be studied through the hyperpolarizability and ΔE values of Na^+(C222)M2 (M2 = Be, Mg & K) series. Hyperpolarizability of Na^+(C222)M2 series increases like, Na^+(C222)Mg^- (2.7×10^5 au) > Na^+(C222)Ca^- (2.0×10^5 au) > Na^+(C222)Be^- (6.5×10^4 au) while ΔE shows the decreasing trend in the same pattern *i.e.,* Na^+(C222)Mg^- (0.68 eV) < Na^+(C222)Ca^- (0.77 eV) < Na^+(C222)Be^- (2.06 eV). Such a trend where ΔE is lowering down a series, is because enlargement of an atom's size (alkaline earth metal here) decreases its ionization potential that ultimately lowers energy required for electronic excitation.

The direct relation between oscillator strength and hyperpolarizability is shown by one of the series *i.e.,* Li series (Li^+(C222)M2). β_o of Li^+(C222)Ca^- (1.3×10^5 au) > Li^+(C222)Mg^- (1.0×10^5 au) > Li^+(C222)Be^- (2.4×10^4 au) and in the same pattern, f_o of Li^+(C222)Ca^- (0.11) > Li^+(C222)Mg^- (0.10) > Li^+(C222)Be^- (0.07).

Moreover, the direct relation between β_o, hyperpolarizability and Δμ, change in dipole moment can be observed in the Na series (Na^+(C222)M2), where the highest value of β_o (2.7×10^5 au) is calculated for the compound Na^+(C222)Mg^- having highest Δμ (5.81 D) as well.

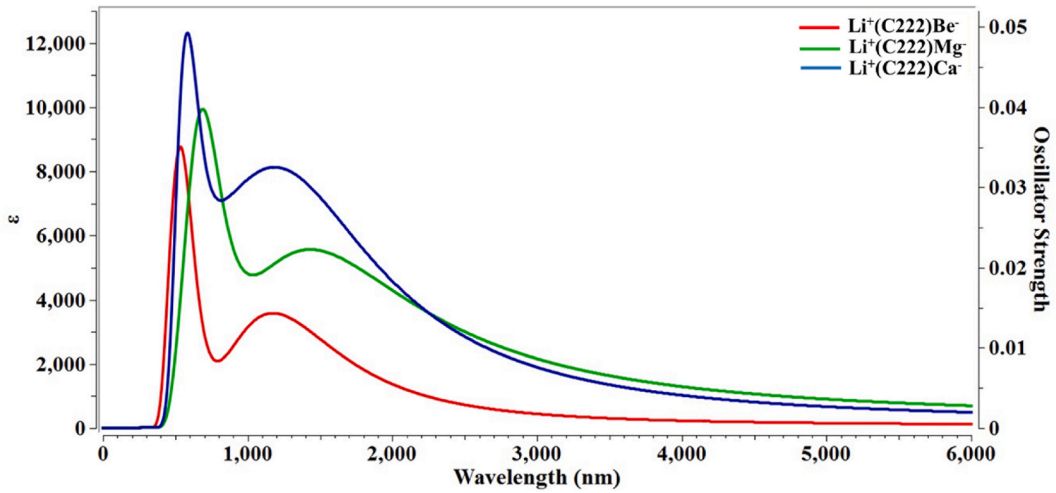

Fig. 5. The UV–VIS absorption spectra of M1(C222)M2 (M1 = Li) (M2 = Be, Mg and Ca) compounds.

3.5. Absorption analysis

Absorption analysis shows the maximum absorption in infrared region. Li series, (Li^+(C222)M2) shows the absorption maxima for Li(C222)Be^- at 1256 nm. A red shift is observed for Li^+(C222)Mg^- to 1614 nm then a slight blue shift is seen for the next compound of the series (Li^+(C222)Ca^-) to 1506 nm. The highest absorption maxima in this series for Li^+(C222)Mg^- can be due to the lowest ΔE of this complex in Li series. A very similar trend is shown by Na^+(C222)M2 and K^+(C222)M2 series. For Na^+(C222)M2 series, an increase in the absorption maxima (λ_{max}) has been observed from Na^+(C222)Be^- (600 nm) to Na^+(C222)Mg^- (1800 nm) then a slight blue shift is seen for the next compound of the series (Na^+(C222)Ca^-) at 1609 nm. Here, the highest absorption maxima showing complex Na^+(C222)Mg^- possesses the lowest ΔE in the series (like Li series) and H-L gap for the same complex is also lowest in the series. For K^+(C222)M2 series, an increase in the absorption maxima (λ_{max}) has been observed from K^+(C222)Be^- (614 nm) to K^+(C222)Mg^- (1796 nm) then a slight blue shift is seen for the next compound of series (K^+(C222)Ca^-) at 1598 nm. Here, the highest absorption maxima showing complex K^+(C222)Mg^- possesses the lowest ΔE in the series (like Li and Na series) and H-L gap for the same complex is also lowest in the series. Spectra are given in Fig. 5/Fig. S3.

4. Effect of EEF on M1(C222)M2

After finding the NLO response of M1(C222)M2 series we took a step forward and aligned the compounds with respect to Cartesian axis using VMD (visual molecular dynamics) software in order to apply the EEF in right direction i.e. ± x, y, z axis (Fig. 6). This results

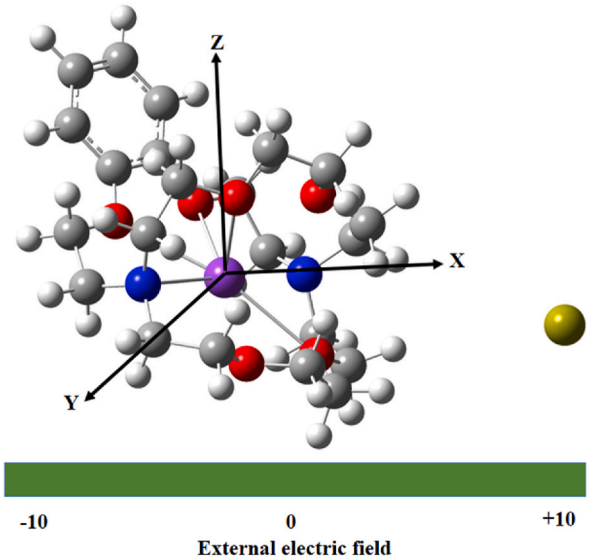

Fig. 6. Geometric structure of M1(C222)M2 under EEF, the Cartesian axis, and direction of positive and negative EEF ($\pm 1 \times 10^{-3}$ au) are presented.

Table 3
Comparison of NBO charges of M1(C222)M2 compounds without EEF and with $\pm 1 \times 10^{-3}$ au EEF.

M1(C222)M2	EEF = 0		EEF = $\pm 1 \times 10^{-3}$		EEF = 0	EEF = $\pm 1 \times 10^{-3}$
	Q^+	Q^-	Q^+	Q^-	$E_{(HOMO-LUMO)}$	$E_{(HOMO-LUMO)}$
Li^+(C222)Be^-	0.57	−0.81	0.85	−0.71	2.83	2.54
Li^+(C222)Mg^-	0.57	−0.83	−0.31	0.01	2.53	1.65
Li^+(C222)Ca^-	0.84	−0.77	−0.01	0.01	2.37	1.47
Na^+(C222)Be^-	0.62	−0.83	0.86	−0.73	2.56	2.26
Na^+(C222)Mg^-	0.87	−0.77	0.85	−0.72	2.26	1.80
Na^+(C222)Ca^-	0.86	−0.78	0.85	−0.73	2.26	1.83
K^+(C222)Be^-	0.64	−0.85	0.88	−0.74	2.29	2.06
K^+(C222)Mg^-	0.60	−0.83	0.01	0.01	2.23	1.93
K^+(C222)Ca^-	0.87	−0.77	0.03	−0.01	2.24	1.46

Table 4
Comparison of mean polarizibility and hyperpolarizability of M1(C222)M2 compounds without EEF and with $\pm 1 \times 10^{-3}$ au EEF.

M1(C222)M2	EEF = 0		EFF = $\pm 1 \times 10^{-3}$	
	α_o	β_o	α_o	β_o
Li^+(C222)Be^-	480	2.41×10^4	493	9.72×10^4
Li^+(C222)Mg^-	644	1.11×10^5	1409	6.87×10^6
Li^+(C222)Ca^-	735	1.35×10^5	1525	6.56×10^6
Na^+(C222)Be^-	492	6.34×10^4	526	2.07×10^5
Na^+(C222)Mg^-	680	2.73×10^5	564	1.89×10^6
Na^+(C222)Ca^-	766	2.01×10^5	966	1.55×10^6
K^+(C222)Be^-	507	4.83×10^4	551	2.90×10^5
K^+(C222)Mg^-	693	1.15×10^5	1023	1.53×10^6
K^+(C222)Ca^-	422	8.79×10^4	5431	2.48×10^7

the application of EEF along the charge transfer direction i.e. M1→M2 and opposite to direction of charge transfer i.e. M2→M1 (M1 = Li, Na, K and M2 = Be, Mg, Ca). Then we run NBO, FMO and hyperpolarizability analysis in the presence of 0.001 au external electric field to find the change in charge transfer, HOMO-LUMO energy gap and hyperpolarizability. Meanwhile we got interesting results which are shown in Tables 3 and 4.

Table 4 shows that there is linear change in the hyperpolarizability of M1(C222)M2 compounds under the influence of applied EEF. The maximum increase is observed in case of K^+(C222)Ca^- where hyperpolarizability has been enhanced from 8.79×10^4 au to 2.48×10^7 au This huge change in the hyperpolarizability can be attributed by the fact that hyperpolarizability increases with decreased HOMO-LUMO energy gap (citation). So, we can infer that EEF can be a good source to design the NLO compounds with maximum hyperpolarizability.

5. Conclusions

In summary, with the help of *ωB97X-D* (6-31+G(d,p)), a new series of alkaline earthides based on Cryptand [222] is designed theoretically and investigated in detail. The compounds bear negative charges and HOMOs reposing over the alkaline earth metals that is examined through NBO and FMO analyses, respectively and is validated through the spectra of partial density of states. Moreover, these properties render these complexes with very small values of transition energies lying in the range of 0.68–2.06 eV. All these characteristic features ultimately result in high hyperpolarizability values ranging from 2.4×10^4 au to 2.7×10^5 au (the largest being calculated to be 2.7×10^5 au for Na^+(C222)Mg^-). Furthermore, applying external electric field on the complexes enhances the hyperpolarizability further by 10 folds. A remarkable increase of 1000 folds has been seen when hyperpolarizability of K^+(C222)Ca^- is calculated after EEF application *i.e.*, from 8.79×10^4 au to 2.48×10^7 au; when subjected to 0.001 au external electric field.

Author contribution statement

Annum Ahsan, Faiza Fayyaz, Sehrish Sarfaraz: Performed the experiments; Analyzed and interpreted the data; Wrote the paper.

Malai Haniti S. A. Hamid, Natasha A. Keasberry: Analyzed and interpreted the data; Contributed reagents, materials, analysis tools or data; Wrote the paper.

Khurshid Ayub, Nadeem S. Sheikh: Conceived and designed the experiments; Analyzed and interpreted the data; Wrote the paper.

Data availability statement

Data included in article/supp. material/referenced in article.

Declaration of competing interest

The authors declare that they have no known competing financial interests or personal relationships that could have appeared to influence the work reported in this paper.

Acknowledgments

The authors thank the Universiti Brunei Darussalam, Brunei Darussalam for the research grant (UBD/RSCH/1.4/FICBF(b)/2022/049) and the allied research grant.

Appendix A. Supplementary data

Supplementary data to this article can be found online at https://doi.org/10.1016/j.heliyon.2023.e17610.

References

[1] N. Issaoui, et al., Combined experimental and theoretical studies on the molecular structures, spectroscopy, and inhibitor activity of 3-(2-thienyl) acrylic acid through AIM, NBO, FT-IR, FT-Raman, UV and HOMO-LUMO analyses, and molecular docking, J. Mol. Struct. 1130 (2017) 659–668.
[2] S. Muhammad, et al., Role of a singlet diradical character in carbon nanomaterials: a novel hot spot for efficient nonlinear optical materials, Nanoscale 8 (42) (2016) 17998–18020.
[3] S. Winter, et al., Back to the roots: photodynamic inactivation of bacteria based on water-soluble curcumin bound to polyvinylpyrrolidone as a photosensitizer, Photochem. Photobiol. Sci. 12 (10) (2013) 1795–1802.
[4] S. Muhammad, M. Nakano, Computational strategies for nonlinear optical properties of carbon nano-systems, Nanoscience and Computational Chemistry: Research Progress 309 (2013).
[5] S. Trabelsi, et al., Synthesis and physic-chemical properties of a novel chromate compound with potential biological applications, bis (2-phenylethylammonium) chromate (VI), J. Mol. Struct. 1185 (2019) 168–182.
[6] A. Sagaama, et al., Non covalent interactions and molecular docking studies on morphine compound, J. King Saud Univ. Sci. 33 (8) (2021), 101606.
[7] A. Ramalingam, et al., Study of a new piperidone as an anti-Alzheimer agent: molecular docking, electronic and intermolecular interaction investigations by DFT method, J. King Saud Univ. Sci. 33 (8) (2021), 101632.
[8] S. Ju, et al., Nonlinear optical properties of zinc doped germano-silicate glass optical fiber, J. Nonlinear Opt. Phys. Mater. 19 (4) (2010) 791–799.
[9] B.G. Kushner, J.A. Neff, Nonlinear Optical Materials & DoD Device Requirements, MRS Online Proceedings Library (OPL), 1987, p. 109.
[10] T. Jiang, et al., Passively Q-switched erbium-doped fiber laser based on gold nanorods, Optik 125 (19) (2014) 5789–5793.
[11] Y. Wang, et al., Four-wave mixing microscopy of nanostructures, Adv. Opt Photon 3 (1) (2011) 1–52.
[12] P. Ren, H. Fan, X. Wang, Electrospun nanofibers of ZnO/BaTiO3 heterostructures with enhanced photocatalytic activity, Catal. Commun. 25 (2012) 32–35.
[13] C. Tang, et al., Two-photon absorption and optical power limiting properties of ladder-type tetraphenylene cored chromophores with different terminal groups, J. Mater. Chem. C 1 (9) (2013) 1771–1780.
[14] K.N. Chopra, A short note on technical analysis of excimer lasers, their optimization for laser corneal refractive surgery, and novel applications, Latin Am. J. Phys. Educ. 8 (4) (2014) 8.
[15] M. Nakano, et al., Second hyperpolarizability (γ) of singlet diradical system: dependence of γ on the diradical character, J. Phys. Chem. 109 (5) (2005) 885–891.
[16] M. Nakano, et al., Second hyperpolarizabilities of polycyclic aromatic hydrocarbons involving phenalenyl radical units, Chem. Phys. Lett. 418 (1–3) (2006) 142–147.
[17] J. Abe, et al., Theoretical study of hyperpolarizabilities of spirolinked Push− pull polyenes, J. Phys. Chem. 101 (1) (1997) 1–4.
[18] Y. Li, et al., Excellent infrared nonlinear optical crystals BaMO (IO3) 5 (M= V, Ta) predicted by first principle calculations, Materials 11 (10) (2018) 1809.
[19] Y. Liu, et al., Structure-property relationship in nonlinear optical materials with π-conjugated CO3 triangles, Coord. Chem. Rev. 407 (2020), 213152.
[20] Y. Liu, et al., Chiral octupolar metal–organoboron NLO frameworks with (14, 3) topology, Angew. Chem. 120 (24) (2008) 4614–4617.
[21] R.-L. Zhong, et al., Role of excess electrons in nonlinear optical response, J. Phys. Chem. Lett. 6 (4) (2015) 612–619.
[22] N. Kosar, et al., Theoretical study on novel superalkali doped graphdiyne complexes: unique approach for the enhancement of electronic and nonlinear optical response, J. Mol. Graph. Model. 97 (2020), 107573.
[23] H. Nistazakis, et al., BER estimation for multi-hop RoFSO QAM or PSK OFDM communication systems over gamma gamma or exponentially modeled turbulence channels, Opt Laser. Technol. 64 (2014) 106–112.
[24] N. Kosar, et al., Doping superalkali on Zn12O12 nanocage constitutes a superior approach to fabricate stable and high-performance nonlinear optical materials, Opt Laser. Technol. 120 (2019), 105753.
[25] F. Ullah, et al., Superalkalis as a source of diffuse excess electrons in newly designed inorganic electrides with remarkable nonlinear response and deep ultraviolet transparency: a DFT study, Appl. Surf. Sci. 483 (2019) 1118–1128.
[26] G. Yu, et al., Theoretical insights and design of intriguing nonlinear optical species involving the excess electron, Int. J. Quant. Chem. 115 (11) (2015) 671–679.
[27] J.-J. Wang, et al., A new strategy for simultaneously enhancing nonlinear optical response and electron stability in novel cup–saucer+–cage−-shaped sandwich electride molecules with an excess electron protected inside the cage, Dalton Trans. 44 (9) (2015) 4207–4214.
[28] M. Miyakawa, et al., Superconductivity in an Inorganic Electride 12CaO⊙ 7Al2O3: e, J. Am. Chem. Soc. 129 (23) (2007) 7270–7271.
[29] Y. Li, et al., An ab initio prediction of the extraordinary static first hyperpolarizability for the electron-solvated cluster (FH) 2 {e}(HF), J. Phys. Chem. B 108 (10) (2004) 3145–3148.
[30] W. Chen, et al., The static polarizability and first hyperpolarizability of the water trimer anion: ab initio study, J. Chem. Phys. 121 (21) (2004) 10489–10494.
[31] K. Ayub, Are phosphide nano-cages better than nitride nano-cages? A kinetic, thermodynamic and non-linear optical properties study of alkali metal encapsulated X 12 Y 12 nano-cages, J. Mater. Chem. C 4 (46) (2016) 10919–10934.
[32] F. Ullah, et al., Design of novel superalkali doped silicon carbide nanocages with giant nonlinear optical response, Opt Laser. Technol. 122 (2020), 105855.
[33] A.S. Rad, K. Ayub, Nonlinear optical and electronic properties of Cr-, Ni-, and Ti-substituted C20 fullerenes: a quantum-chemical study, Mater. Res. Bull. 97 (2018) 399–404.
[34] M.J. Wagner, J.L. Dye, [Cs+ (15-crown-5)(18-crown-6) e-] 6·(18-crown-6): properties of the first mixed crown ether electride, J. Solid State Chem. 117 (2) (1995) 309–317.
[35] R. Huang, et al., Structure of K+ (cryptand [2.2. 2J) electride and evidence for trapped electron pairs, Nature 331 (6157) (1988) 599–601.
[36] A.S. Ichimura, M.J. Wagner, J.L. Dye, Anisotropic charge transport and Spin− spin interactions in K+ (cryptand [2.2. 2]) electride, J. Phys. Chem. B 106 (43) (2002) 11196–11202.
[37] M.J. Wagner, et al., An electride with a large six-electron ring, Nature 368 (6473) (1994) 726–729.

[38] M.Y. Redko, et al., Design and synthesis of a thermally stable organic electride, J. Am. Chem. Soc. 127 (35) (2005) 12416–12422.
[39] W. Chen, et al., The structure and the large nonlinear optical properties of Li@ Calix [4] pyrrole, J. Am. Chem. Soc. 127 (31) (2005) 10977–10981.
[40] X. Li, Design of novel graphdiyne-based materials with large second-order nonlinear optical properties, J. Mater. Chem. C 6 (28) (2018) 7576–7583.
[41] W.M. Sun, et al., Stability and nonlinear optical response of alkalides that contain a completely encapsulated superalkali cluster, ChemPhysChem 17 (17) (2016) 2672–2678.
[42] X.-H. Li, et al., Designing a new class of excess electron compounds with unique electronic structures and extremely large non-linear optical responses, New J. Chem. 44 (16) (2020) 6411–6419.
[43] W.-M. Sun, et al., On the potential application of superalkali clusters in designing novel alkalides with large nonlinear optical properties, Inorg. Chem. 53 (12) (2014) 6170–6178.
[44] W.-M. Sun, et al., Theoretical study on superalkali (Li 3) in ammonia: novel alkalides with considerably large first hyperpolarizabilities, Dalton Trans. 43 (2) (2014) 486–494.
[45] W.-M. Sun, et al., A theoretical study on novel alkaline earth-based excess electron compounds: unique alkalides with considerable nonlinear optical responses, Phys. Chem. Chem. Phys. 17 (6) (2015) 4524–4532.
[46] F.-F. Wang, et al., Structures and considerable static first hyperpolarizabilities: new organic alkalides (M+@ n 6adz) M '-(M, M '= Li, Na, K; n= 2, 3) with cation inside and anion outside of the cage complexants, J. Phys. Chem. B 112 (4) (2008) 1090–1094.
[47] W. Chen, et al., Nonlinear optical properties of alkalides Li+ (calix [4] pyrrole) M-(M= Li, Na, and K): alkali anion atomic number dependence, J. Am. Chem. Soc. 128 (4) (2006) 1072–1073.
[48] J. Hou, et al., Alkaline-earthide: a new class of excess electron compounds Li-C6H6F6-M (M= Be, Mg and Ca) with extremely large nonlinear optical responses, Chem. Phys. Lett. 711 (2018) 55–59.
[49] A. Ahsan, K. Ayub, Extremely large nonlinear optical response and excellent electronic stability of true alkaline earthides based on hexaammine complexant, J. Mol. Liq. 297 (2020), 111899.
[50] A. Ahsan, et al., Theoretical study of 36Adz based alkaline earthides M+ (36Adz) M−(M+= Li & Na; M−= Be, Mg & Ca) with remarkable nonlinear optical response, Mater. Sci. Semicond. Process. 153 (2023), 107119.
[51] A. Ahsan, K. Ayub, Adamanzane based alkaline earthides with excellent nonlinear optical response and ultraviolet transparency, Opt Laser. Technol. 129 (2020), 106298.
[52] A. Ahsan, et al., Enhanced non-linear optical response of calix [4] pyrrole complexant based earthides in the presence of oriented external electric field, J. Mol. Liq. 350 (2022), 118504.
[53] A. Ahsan, et al., Alkaline earthides based on 15-crown-5 ether with remarkable NLO response, Eur. Phys. J. Plus 137 (10) (2022) 1149.
[54] J.L. Dye, Electrides: early examples of quantum confinement, Accounts Chem. Res. 42 (10) (2009) 1564–1572.
[55] H.-J. Buschmann, The macrocyclic and cryptate effect. 8. Complex formation of the cryptands (222),(222B),(222BB) and (222CC) with different cations in methanol solutions, Inorg. Chim. Acta. 134 (2) (1987) 225–228.
[56] M. Hiraoka, Crown Ethers and Analogous Compounds, Elsevier, 2016.
[57] A.K. Srivastava, External electric field modulated second-order nonlinear optical response and visible transparency in hexalithiobenzene, J. Mol. Model. 27 (2) (2021) 1–8.
[58] B. Li, et al., A nonlinear optical switch induced by an external electric field: inorganic alkaline–earth alkalide, RSC Adv. 9 (29) (2019) 16718–16728.
[59] M. Savarese, E. Bremond, C. Adamo, Exploring the limits of recent exchange–correlation functionals in modeling lithium/benzene interaction, Theor. Chem. Acc. 135 (4) (2016) 1–11.
[60] S. Grimme, et al., A consistent and accurate ab initio parametrization of density functional dispersion correction (DFT-D) for the 94 elements H-Pu, J. Chem. Phys. 132 (15) (2010), 154104.
[61] S. Grimme, Accurate description of van der Waals complexes by density functional theory including empirical corrections, J. Comput. Chem. 25 (12) (2004) 1463–1473.
[62] L. Xu, A. Kumar, B.M. Wong, Linear polarizabilities and second hyperpolarizabilities of streptocyanines: results from broken-Symmetry DFT and new CCSD (T) benchmarks, J. Comput. Chem. 39 (28) (2018) 2350–2359.
[63] H.-Q. Wang, et al., A thorough understanding of the nonlinear optical properties of BODIPY/carborane/diketopyrrolopyrrole hybrid chromophores: module contribution, linear combination, one-/two-dimensional difference and carborane's arrangement, J. Mater. Chem. C 7 (25) (2019) 7531–7547.
[64] H.-Q. Wang, et al., Multinuclear "staircase" oligomers based on the (Et2C2B4H4) Fe (η6-C6H6) sandwich unit: quantitative tailorable and redox switchable nonlinear optics, J. Phys. Chem. C 121 (30) (2017) 16470–16480.
[65] H.-Q. Wang, et al., Planar octagonal tetranuclear cobaltacarborane macrocycle [(η5-C5Me5) Co (2, 3-Et2C2B4H3-5-C□ C-7-C□ C)] 4 for 2D nonlinear optics: ultra-high-response and multistate controlled cubic NLO switch, J. Phys. Chem. C 121 (51) (2017) 28462–28474.
[66] F. Ullah, K. Ayub, T. Mahmood, Remarkable second and third order nonlinear optical properties of organometallic C 6 Li 6–M 3 O electrides, New J. Chem. 44 (23) (2020) 9822–9829.
[67] S. Wajid, et al., Demonstrating the potential of alkali metal-doped cyclic C6O6Li6 organometallics as electrides and high-performance NLO materials, ACS Omega 6 (44) (2021) 29852–29861.
[68] N. Kosar, K. Ayub, T. Mahmood, Surface functionalization of twisted graphene C32H15 and C104H52 derivatives with alkalis and superalkalis for NLO response; a DFT study, J. Mol. Graph. Model. 102 (2021), 107794.
[69] J. Iqbal, K. Ayub, Theoretical study of the non linear optical properties of alkali metal (Li, Na, K) doped aluminum nitride nanocages, RSC Adv. 6 (96) (2016) 94228–94235.
[70] M.B.n. Oviedo, N.V. Ilawe, B.M. Wong, Polarizabilities of π-conjugated chains revisited: improved results from broken-symmetry range-separated DFT and new CCSD (T) benchmarks, J. Chem. Theor. Comput. 12 (8) (2016) 3593–3602.
[71] L.L. Beecroft, C.K. Ober, Nanocomposite materials for optical applications, Chem. Mater. 9 (6) (1997) 1302–1317.
[72] S. Grimme, Semiempirical GGA-type density functional constructed with a long-range dispersion correction, J. Comput. Chem. 27 (15) (2006) 1787–1799.
[73] R.A. Gaussian09, 1, mj frisch, gw trucks, hb schlegel, ge scuseria, ma robb, jr cheeseman, g. Scalmani, v. Barone, b. Mennucci, ga petersson et al, vol. 121, *gaussian.* Inc., Wallingford CT, 2009, pp. 150–166.
[74] S. Khan, et al., First-principles study for exploring the adsorption behavior of G-series nerve agents on graphdyine surface, Computational and Theoretical Chemistry 1191 (2020), 113043.
[75] T. Lu, F. Chen, Multiwfn: a multifunctional wavefunction analyzer, J. Comput. Chem. 33 (5) (2012) 580–592.
[76] W.-M. Sun, et al., Can coinage metal atoms Be capable of serving as an excess electron source of alkalides with considerable nonlinear optical responses? Inorg. Chem. 56 (8) (2017) 4594–4600.
[77] S. Muhammad, Quantum chemical design of triple hybrid organic, inorganic and organometallic materials: an efficient two-dimensional second-order nonlinear optical material, Mater. Chem. Phys. 220 (2018) 286–292.
[78] W.-M. Sun, et al., Designing magnetic superalkalis with extremely large nonlinear optical responses, Organometallics 41 (17) (2022) 2406–2414.
[79] W.-M. Sun, et al., Designing alkalides with considerable nonlinear optical responses and high stability based on the facially polarized janus all-cis-1, 2, 3, 4, 5, 6-hexafluorocyclohexane, Organometallics 36 (17) (2017) 3352–3359.
[80] W.-M. Sun, et al., A theoretical study on superalkali-doped nanocages: unique inorganic electrides with high stability, deep-ultraviolet transparency, and a considerable nonlinear optical response, Dalton Trans. 45 (17) (2016) 7500–7509.